Annals of Nuclear Cardiology Vol. 2 No. 1 111−121

FOCUS ISSUE: MBF QUANTIFICATION−REVIEW ARTICLE

Quantitative Assessment of Regional Myocardial Blood Flow with Clinical SPECT

Hidehiro Iida, PhD, DSc[1)], Hirotaka Maruno, MD[2)], Kazuhiro Koshino, PhD[1)], Saeka Shimochi, MSC, DVM[1)], Takashi Temma, PhD[1)], Brian F. Hutton, PhD[3)] and Shinro Matsuo, MD, PhD[4)]

Received: July 6, 2016/Revised manuscript received: July 27, 2016/Accepted: July 29, 2016

Abstract

This article gives an overview of essential requirements and limitations in the quantitative assessment of regional myocardial perfusion or regional myocardial blood flow (rMBF) using existing clinical SPECT systems in clinical settings. One major requirement is the need for acquiring complete projection data without truncation. Attenuation and scatter are then prerequisites to reproduce quantitative images which should represent regional distribution of true radioactivity concentration in the myocardium. A compartmental model could then be applied to extract physiological myocardial perfusion from series of tomographic images acquired following i.v. radio ligand administration. There are also requirements in the radio-ligands if one wish to estimate quantitative blood flow for a physiologicaly wide range of flow. The most important factor is need for a high first-pass extraction fraction. Several factors that affect quantitative ability are reviewed and their importance is illustrated by example.

Keywords: Blood flow, Kinetic model, Quantification, SPECT
Ann Nucl Cardiol 2016；2（1）：111-121

Single-photon-emission computed tomography (SPECT) can provide myocardial images reflecting bio-physiologic function in vivo, such as regional perfusion, metabolism of several substrates, and the binding potential of given ligands to particular receptors. Although planar imaging was used previously to evaluate coronary flow reserve, quantitative assessment by SPECT is not fully established. Therefore, this article describes future perspectives, and essential requirements and limitations, for the quantitative assessment of regional myocardial perfusion or regional myocardial blood flow (rMBF) using clinical SPECT systems.

Quantitative SPECT reconstruction

Quantitative SPECT reconstruction should result in tomographic images where voxel values are proportional to the true distribution of radio-ligand concentrations at every temporal period. Mathematical kinetic models can be applied to estimate physiological functional images, as is established in positron emission tomography (PET). Practical requirements in SPECT have extensively been discussed in earlier articles (1, 2). Despite a relatively long history of cardiac SPECT imaging, there have been only limited attempts to quantitatively assess physiologic parameters. This is largely attributed to the limited sensitivity and resolution of SPECT devices as compared with PET, and the complexity of attenuation and scatter correction for SPECT, particularly in the heterogeneous thorax (Fig. 1). In addition, general use of filtered back projection reconstruction for data collected with 180° views to improve qualitative image appearance does not lend itself well to quantitative studies.

In brain, SPECT has been well accepted for assessing quantitative parametric images of cerebral perfusion (3,4) and

doi：10.17996/ANC.02.01.111

1) Hidehiro Iida, Kazuhiro Koshino, Saeka Shimochi, Takashi Temma
Department of Investigative Radiology, National Cerebral & Cardiovascular Research Center - Research Institute, 5-7-1 Fujishiro-dai, Suita City, Osaka, Japan 565-8565
E-mail: iida@ri.ncvc.go.jp
2) Hirotaka Maruno
Department of Radiation Oncology and Nuclear Medicine, Toranomon Hospital, Tokyo, Japan
3) Brian F. Hutton
Institute of Nuclear Medicine, University College London, London, U.K.
4) Shinro Matsuo
Department of Nuclear Medicine, Kanazawa University Hospital, Ishikawa, Japan

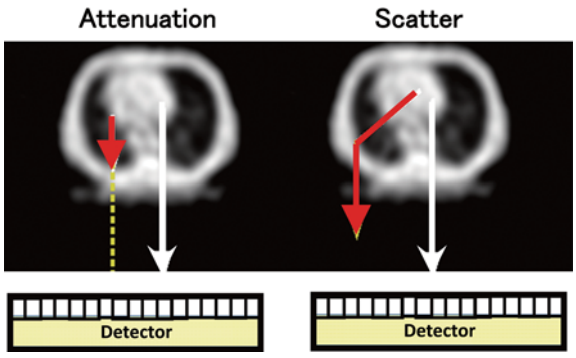

Fig. 1
Illustration of attenuation and scatter in SPECT. Attenuation causes a reduction in measured counts, particularly in deep structures, while scatter causes mis-positioning of detected counts. Both effects have to be accurately corrected for quantitative regional activity measurement.

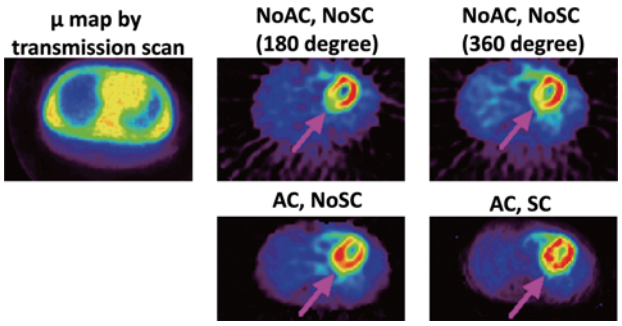

Fig. 2
Comparison of tomographic images obtained from a typical normal volunteer (22-year-old male) after ^{201}T1 injection. In the image without attenuation or scatter correction (NoAC. NoSC), radioactivity is clearly underestimated in the posterior wall region. Attenuation correction (AC using a measured μ-map obtained from the transmission CT (TCT), but without scatter correction (AC, NoSC), overcompensated for attenuation in the posterior region, causing an apparent anterior wall defect. When both attenuation and scatter corrections are applied with an appropriate μ-map (AC. SC), radioactivity distribution is reasonably homogeneous along the myocardial wall. Figure is reproduced from a reference (2) with modification.

other functions (5-8). Acquisition of 360 degree data with avoidance of truncation is a standard and essential protocol. Appropriate corrections for attenuation and scatter have also been suggested (1,2), in order to provide accurate images. Fig. 2 demonstrates the importance of corrections for both attenuation and scatter, significantly improving quantitative accuracy. In this data, the same methodology has been applied to rMBF quantification, using the same reconstruction as has been utilized for brain (Fig. 3a) (2). Parallel-beam collimated multiple line sources were used in the transmission measurement, and the quantitative μ-value was 0.167 cm^{-1} in the left ventricular chamber for ^{99m}Tc energy range (9). It should be noted that the validation of the performance, particularly the quantitative accuracy, by using various geometrical phantoms containing known radioactivity distributions is important (Fig. 3b). Although much less common, absolute physiological parameter estimation in the myocardium was shown to be feasible using clinical SPECT systems, and has been successfully applied to dynamic ^{201}Tl SPECT to assess quantitative rMBF at rest and after pharmacological challenges (2,9). It is obvious that, because of the need for 360° acquisition and avoidance of truncation, the quantitative reconstruction places additional requirements on the SPECT data collection and processing over current standard clinical protocols. While attenuation correction techniques are well established, care has to be taken in the choice of scatter correction algorithm in order to maintain quantitative accuracy and to avoid artifacts (10) (Fig. 4). A camera capable of performing dynamic SPECT has been required, and the short frame times and relatively poor sensitivity of SPECT require methodology capable of handling the noisy data.

Requirements for the radio-tracer

It should be noted that the limitations in SPECT mentioned above are reflected in the SPECT radiotracer development. Most tracers do not achieve a trans-capillary extraction (first-pass extraction fraction) high enough to support uptake linearly coupled to the true flow, though this is an essential requirement for absolute quantification over a wide physiological range (Fig. 5). Instead, emphasis has been placed on tracers, whose uptake remains relatively constant over the long imaging times typically associated with SPECT, and which provide good contrast between the myocardium and adjacent structures (e.g. liver) allowing delayed imaging when some of the background activity has diminished. Tracers, such as ^{99m}Tc-teboroxime, with properties well suited to measuring perfusion (11-13), but requiring rapid SPECT due to fast clearance, have thus not found widespread use. Although ^{201}Tl is not an ideal radionuclide due to its physical characteristics (low energy of photons resulting in larger amount of attenuation and scatter, poorer resolution and longer half-life of approximately 72 hours resulting in need for reduced activity and consequently poorer count statistics), this ligand is the best in terms of kinetic behavior as a SPECT flow tracer.

Radio-labeled microspheres are considered the gold standard for quantification of rMBF, because their distribution is proportional to the tissue perfusion, and quantitative flow values can be obtained simply from the radioactivity concentration in the tissue divided by the integration of the arterial input function. However, physical microsphere measurements are limited to animal experiments due to their invasive nature. For clinical studies, most SPECT flow tracers are designed to mimic microspheres through relatively high first pass extraction fraction and retention in the tissue by high chemical affinity (or a large tissue-to-blood partition coeffi-

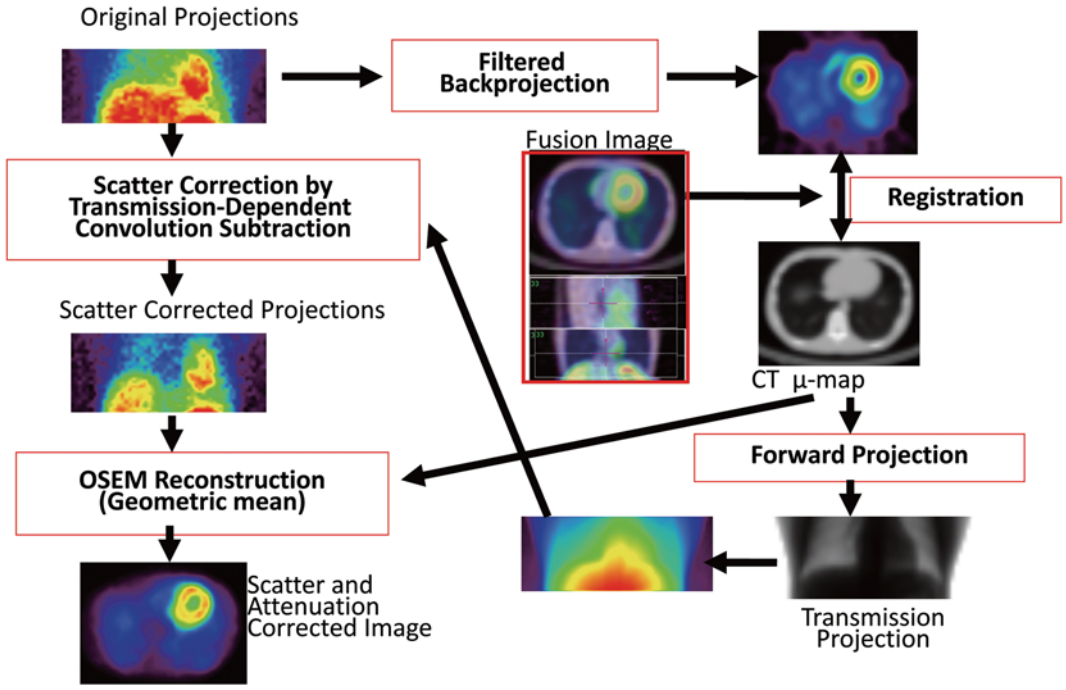

a

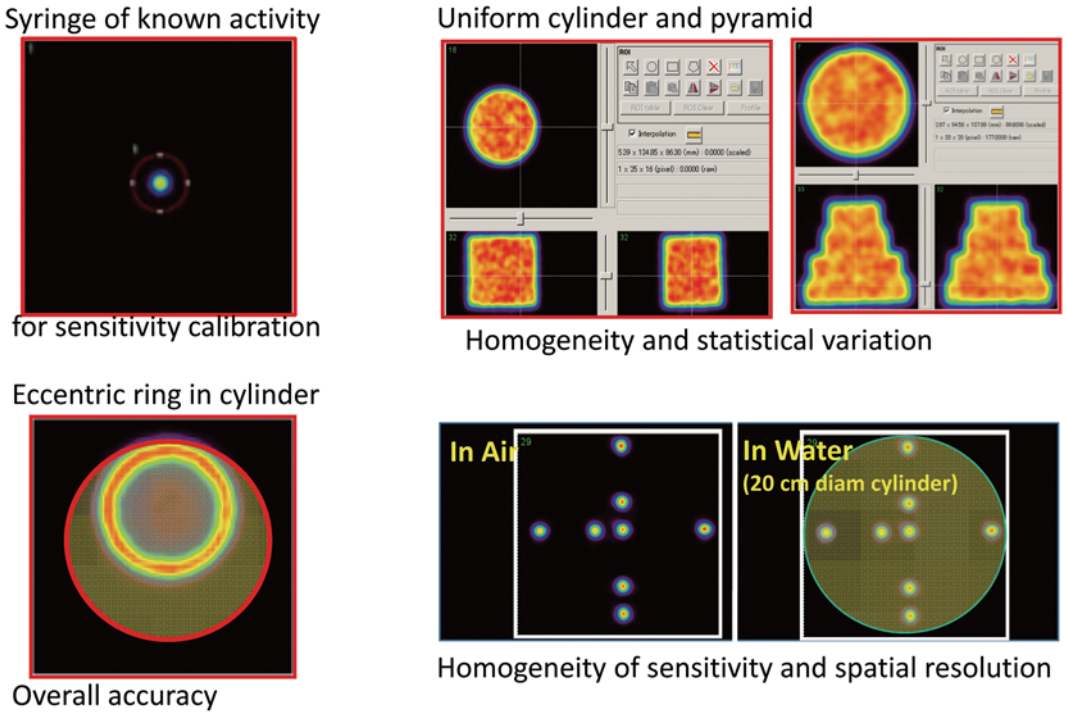

b

Fig. 3

a Schematic diagram of an example SPECT reconstruction software employed in earlier studies to quantitatively assess rMBF using ^{201}Tl (9,23,24). For the reconstruction in the thorax region, CT-derived attenuation μ-images should be provided. Attenuation projection data are generated, from which, together with the emission projection, the scatter projection data is generated. The images are then reconstructed from the scatter-corrected projection data using the ordered-subset expectation-maximization (OSEM) algorithm. The attenuation process is implemented during the OSEM reconstruction using the CT-derived μ-map.

b Example results from a series of physical phantom experiments. By scanning a syringe containing known radioactivity, the reconstructed images are calibrated. Entire radioactivity was then filled to the cylinder phantom, and also to the pyramid phantom. Uniformity and consistency of the radioactivity concentration relative to the syringe radioactivity can be evaluated. Radioactivity was also filled into a cylindrical wall placed eccentrically in the water-filled cylinder phantom. Homogeneity along the ring wall can demonstrate the adequacy of reconstruction procedures including all corrections. Seven line sources are also filled with radioactivity, and spatial resolution, and homogeneity of the radioactivity are evaluated for each source, both in the air, and also in a cylinder filled uniformly with water. A Symbia T6 SPECT scanner fitted with LEHR-parallel collimator was used, and all experiments were performed with ^{99m}Tc.

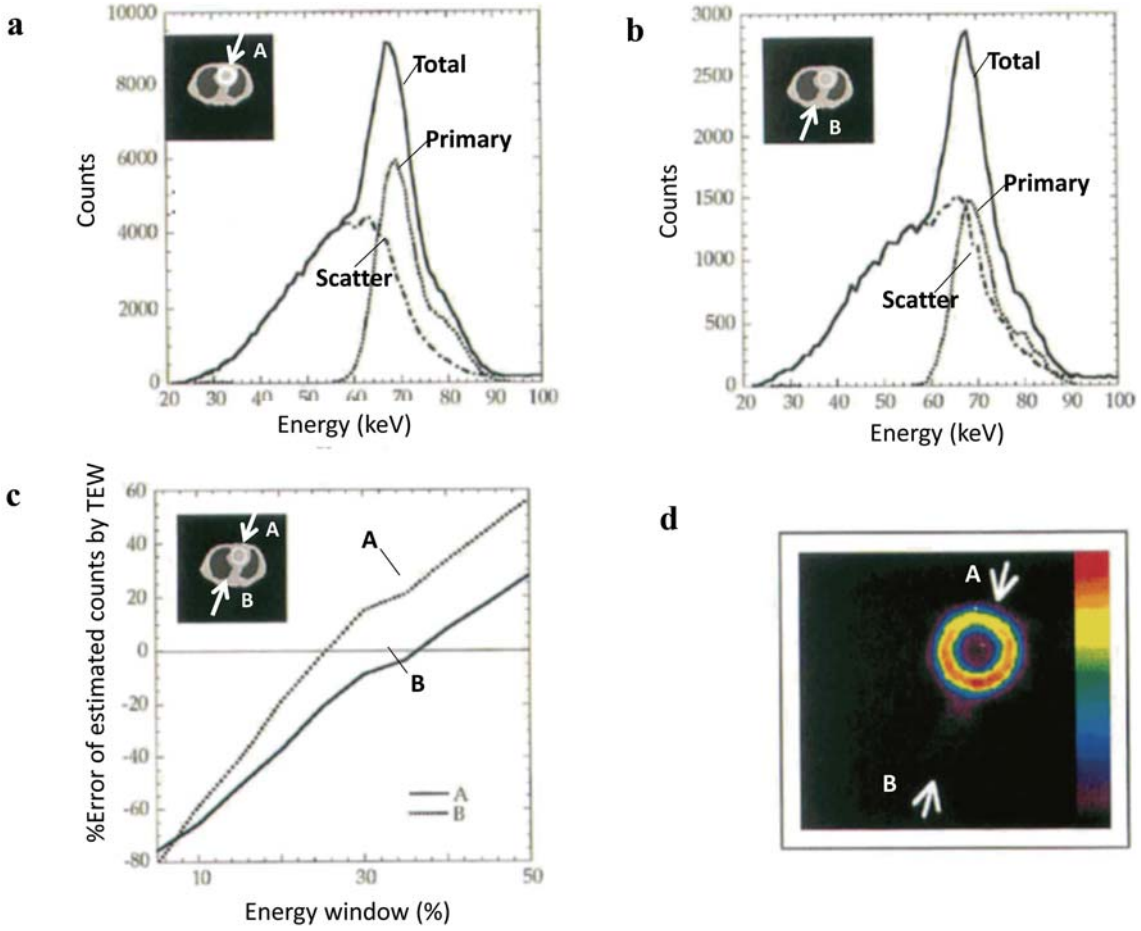

Fig. 4

Results from a Monte-Carlo Simulation on a thorax phantom containing a ring-shape structure with homogeneous radioactivity concentration in the myocardial region. Energy spectra of photo-electric and scattered events from the frontal view, A (a), and from the posterior view, B (b). Scatter-corrected counts estimated by the triple-energy window (TEW) technique for the projection views of A and B is plotted as a function energy window setting in (c). As a result of different amount of scattered events with TEW, the reconstruction failed to reproduce homogeneous myocardial wall (d). See also results from the phantom experiment shown in Fig. 3. Data are from Narita et al. (10).

cient, or distribution volume). However, the fixation of these tracers is often imperfect, and tracers can clear from the tissue during the study period. This causes the regional radioactivity concentration to change over time and no longer entirely reflect flow in delayed images. Retention of the tracer can also be affected by the pathology of the tissue. While the assumption of microsphere-like behavior may be valid in normal tissue, it does not necessarily hold in abnormal myocardial regions.

Change of tracer distribution over time is well demonstrated by ^{201}Tl. It is a potassium analogue, which accumulates in myocardial cells associated with the Na+/K+ ATPase. Because of a high trans-capillary extraction fraction, it is rapidly taken into the myocardial tissue, and initial regional uptake predominantly reflects regional blood flow. ^{201}Tl clears rapidly from arterial blood, reducing delivery of tracer to the myocardium. When an equilibrium is reached between myocardial and blood ^{201}Tl concentration, the myocardial concentration of ^{201}Tl no longer reflects flow, but reflects the myocardium's ability to retain ^{201}Tl and is related to the number of myocytes with maintained membrane potential in a given volume unit (2). Kinetics of ^{201}Tl in myocardial tissue have been extensively studied in the 1970s and early 1980s, and are in fact indirectly applied to clinical studies. In normal myocardium, there is a rapid initial uptake reflecting normal flow, followed by slow clearance toward equilibrium. For ischemic myocardium, with maintained cell potential, initial uptake is low as a result of low flow, and uptake continues toward the same equilibrium as normal myocardium (redistribution). In infarcted areas, reduced flow causes an initial reduced uptake, and loss of cell membrane potential causes loss of ability to retain ^{201}Tl and increased clearance rate, indicating a complete defect. Areas could also have maintained flow with reduced membrane potential, in which the initial uptake is normal, but rapid clearance causes reduced equilibrium tracer concentration (reverse-redistribution). Clinical diagnosis thus involves qualitative (visual) analysis of the early and delayed images. The early images taken at 15-20

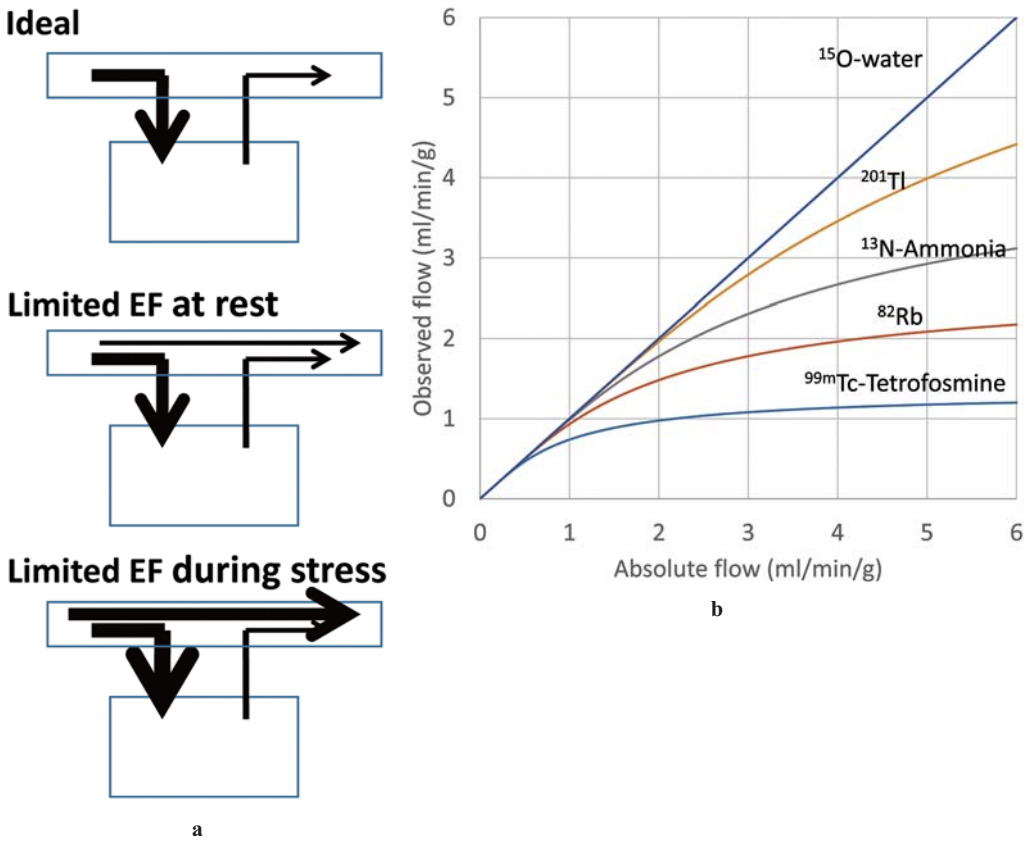

Fig. 5.

a Three situations of radio-ligand uptake to tissue from the capillary bed. In an ideal situation, radio-ligand has the maximum first-pass extraction, so that all activity is transported to the tissue. Thus the uptake rate of the radio-ligand becomes identical to the rate of the tracer supplied to the system, namely the flow rate. In a realistic situation, however, some fraction cannot be transported to the tissue, so that uptake rate is systematically smaller than the flow rate. In this situation, when flow is elevated, the fraction of transport is decreased due to the reduce reaction time through the capillary bed, thus flow can be further underestimated.

b The magnitude of the underestimation in measured flow depends on the flow values; the higher the flow, the more significant the underestimation is. The magnitude of the underestimation also depends on the radio-ligand. ^{99m}Tc-labeled ligands generally do not to have high extraction fraction, thus underestimation is dominant particularly a high flow range. Figures are reproduced from the reference (48), with additional values for ^{201}Tl (49).

minutes demonstrate flow, and the delayed images taken at 3 to 24 hours are used for identifying viable myocardium. There is the potential to quantitatively assess rMBF and the distribution volume (the Na+/K+ potential) from a series of dynamic scans with ^{201}Tl. Previous studies have revealed that both regional blood flow and the distribution volume can be quantitatively estimated by employing quantitative reconstruction including appropriate correction strategies for attenuation and scatter and application of a kinetic mathematical model (2, 9,14).

Kinetic model-based analysis for blood flow quantitation

Kinetic model-based analysis has been well established in PET providing physiological parameter estimates in a quantitative manner. The technique is essentially based on the fitting of kinetic parameters defined by suitable mathematical model formulation to the dynamic data or sequential images acquired following radio-tracer administration. A number of studies demonstrated that rMBF could be readily quantified by means of the kinetic analysis using PET. A typical example was to utilize ^{15}O-water, which included a correction for the partial-volume effect and a determination of the distribution volume of water (or water-perfusable tissue fraction) (15-18), as well as the spillover from the blood activity (17). The method has also been applied to fit quantitative flow values to the empirically validated kinetic model, with other radio-ligands such as ^{13}N-ammonia, ^{82}Rb, etc. Physiological and/or biological processes of the ligand kinetics are often modeled by compartmental assumptions including flow, and retention mechanism.

With appropriate reconstruction procedures for dynamically acquired SPECT images, regional time-activity curves obtained following intravenous injection of ^{201}Tl can reflect quantitative myocardial blood flow, e.g., rapid rise with rapid

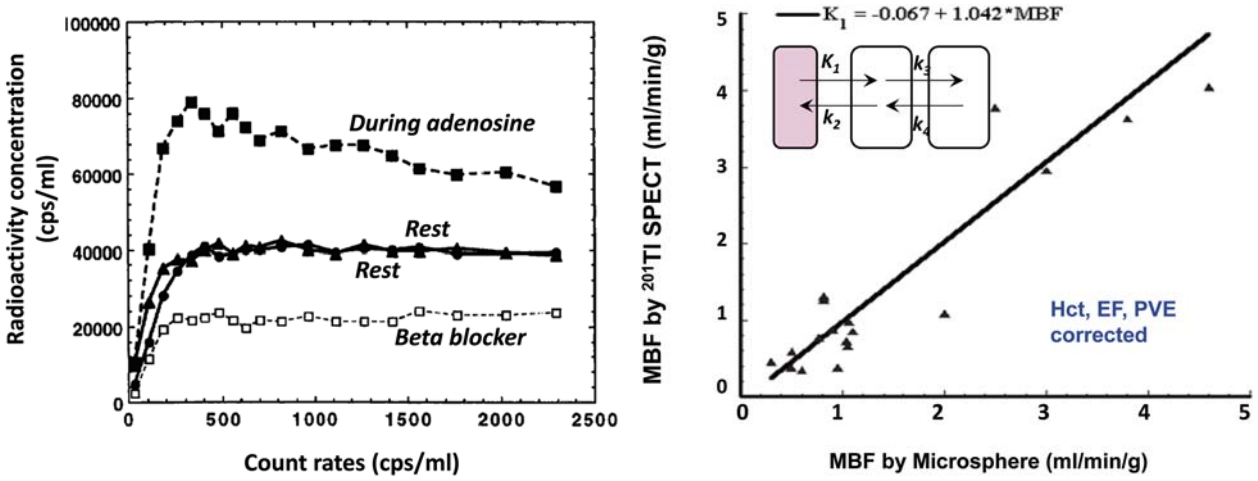

a b

Fig. 6.

a Myocardial time-activity curves obtained from dog experiments after intravenous ^{201}T1 administration at rest (n＝2), during adenosine infusion (n=1), and during β-blocker infusion (n=1). Curves are normalized by the arterial input function integral.

b Comparison of rMBF (MBF) values estimated from kinetic analysis of ^{201}Tl dynamic SPECT data with those determined by the in vitro microsphere method. Agreement of rMBFvalues for a physiologically wide range of blood flows suggests the validity of assessing the quantitative myocardial blood flow using ^{201}TI and SPECT. The three-compartment model is assumed in the kinetic analysis. Corrections were employed for the first-pass extraction fraction, hematocrit (time-dependent change of the plasma-to-whole blood radioactivity concentration ratios in the arterial blood), and the partial volume effect. Figures are reproduced from the reference (9) with modification.

clearance at elevated flow condition, and slower rise and decreased clearance at reduced flow condition as shown in Fig. 6a. It was also shown that compartmental model analysis resulted in quantitative myocardial blood flow values which agreed well with those obtained in canine subjects by invasive radio-microsphere experiments for a physiologically wide range as demonstrated in Fig. 6b. Note that detailed corrections are also needed to compensate for the limited first-pass extraction fraction, and the plasma-to-whole blood ratio of ^{201}Tl concentration. Corrections for partial volume effects, which are caused by the limited spatial resolution, as well as for the additional blurring introduced by cardiac and respiratory motion, also need to be addressed.

Instead of the kinetic fitting approach to estimate quantitative myocardial blood flow, calculation procedures can be reduced by employing simplified techniques, such as a table-look-up technique as has been utilized in perfusion scans in brain SPECT (3,19-22), provided that appropriate validation studies are carried out prior to their applications. Importantly full 360° projection data were acquired for reconstruction, and corrections for both attenuation and scatter were carried out to assure the quantitative accuracy (3). The technique has been applied to myocardial SPECT images acquired soon after intravenous ^{201}Tl injection to estimate rMBF from a single SPECT scan (23). The table-look-up technique is based on the compartment model formulation and it compensates for the reduction of the contrast between the high flow and low flow regions, utilizing a previously determined population-based arterial input function which was calibrated with a single arterial blood sample (23). Maruno et al (24) carried out clinical scans using the same protocol, with and without bicycle ergometer exercise (Fig. 7a). They also showed that quantitative reconstruction plays an important role, if one requires quantitative assessment (Fig. 7b). It was then demonstrated that the absolute myocardial blood flow assessed with the table-look-up approach was significantly higher during the exercise test than that assessed at rest in patients with no evidence of myocardial ischemia or infarction (Fig. 7c), and that the absolute flow values were significantly correlated to the maximum rate-pressure product (RPP) during the bicycle ergometer test (Fig. 7d). These findings suggest the potential of assessing quantitative rMBF in clinical settings. The need for the arterial blood sampling might potentially be avoided, by replacing it by a technique to normalize the injected radioactivity divided by an effective body weight index (23), as tested for brain perfusion studies using ^{123}I-IMP (25). Obviously, further studies should be carried out on much larger patient populations.

Kinetics of ^{99m}Tc-tetrofosmin in a metabolism-perfusion mismatch region

^{99m}Tc-tetrofosmin is a lipophilic cation, whose accumulation into the tissue is attributed to the Na+/H+ ion channel, as well as cellular and mitochondrial membrane potential. Assuming that trans-capillary extraction of ^{99m}Tc-tetrofosmin is high enough and that the extracted ^{99m}Tc-tetrofosmin stays in tissue,

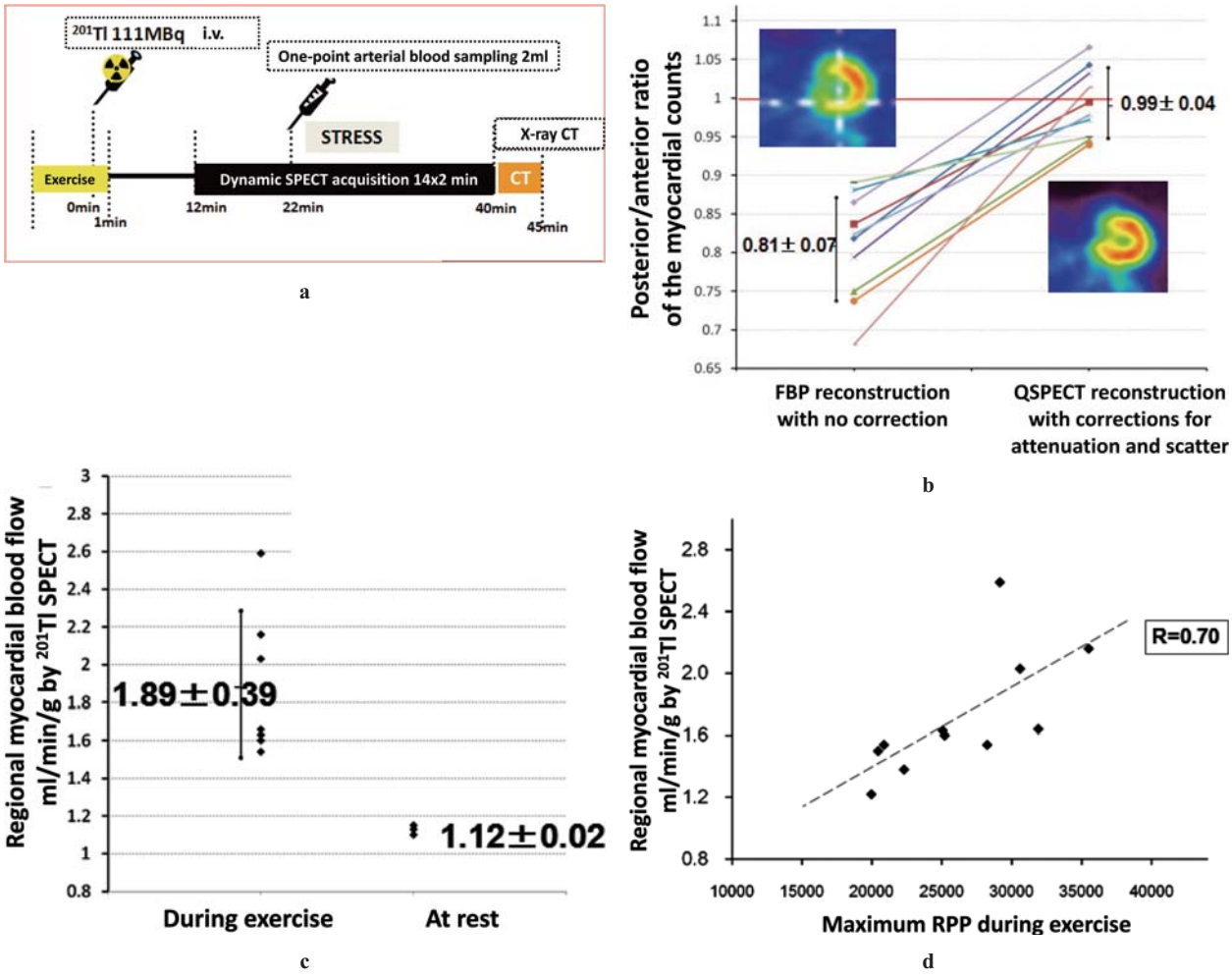

Fig. 7.

a A typical protocol to calculate quantitative rMBF images from a single SPECT scan taken after intra venous injection of ^{201}Tl by means of the table-look-up approach. The technique similar to that used in in vivo autoradiography in quantitative cerebral perfusion scans. Exercise or pharmacological challenges can be given before and during ^{201}Tl injection.

b Impact of quantitative reconstruction on the myocardial images. Posterior-to-frontal count ratios are significantly smaller than unity if correction is not applied for attenuation and scatter. Quantitative reconstruction using the QSPECT software improved and resulted in the count ratio which is not significantly different from unity.

c rMBF was significantly higher when studied during the bicycle ergometer exercise test as compared with at rest, where the exercise was carried out until the heart rate reached 85% or more of the age-predicted maximum value.

d The rMBF values observed demonstrated a significant correlation with the maximum rate-pressure product (RPP) values observed during exercise.

the accumulation rate of ^{99m}Tc-tetrofosmin in tissue has been considered to be identical to the supply rate of this tracer into the capillary bed, and therefore should represent regional flow (26). However, ^{99m}Tc-tetrofosmin uptake can be modified by the Na+/H+ antiporter and mitochondrial un-coupler, suggesting that the ^{99m}Tc-tetrofosmin uptake can be influenced by the membrane potential and mitochondrial integrity (27-30). It was also shown that myocardial ^{99m}Tc-tetrofosmin has a significant washout from the myocardium during the study, even in the normal myocardium at rest (31-33). The clearance of myocardial ^{99m}Tc-tetrofosmin became greater in the reperfused myocardium (34). These findings suggest that the myocardial ^{99m}Tc-tetrofosmin concentration can be influenced not only by myocardial flow but also by energy-dependent processes.

Schaefer et al (35) investigated absolute myocardial blood flow in the area of mismatch between ^{18}F-fluorodeoxyglucose (^{18}FDG) uptake and relative ^{99m}Tc-tetrofosmine uptake, and demonstrated that the rMBF assessed with $H_2{}^{15}O$ PET was preserved in regions with reduced ^{99m}Tc-tetrofosmin uptake and preserved ^{18}F-fluorodeoxyglucose (^{18}FDG), namely the metabolism- perfusion mismatch myocardium (MPMM), as shown in Fig. 8. It is therefore clear that, in clinical situations, like ^{201}Tl, alteration of the energy-dependent cellular membrane potential occurs in regions of MPMM despite preserved resting blood flow, and this is responsible for the reduced uptake of ^{99m}Tc-tetrofosmin. The presence of flow-metabolism mismatch can therefore be significantly overestimated if ^{99m}Tc-

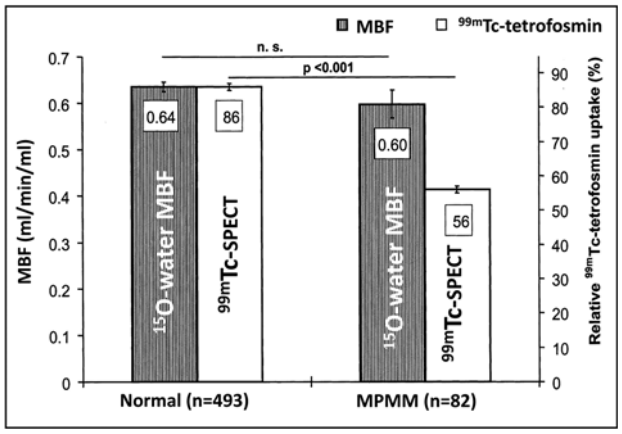

Fig. 8

Comparison of mean myocardial blood flow (MBF) (mL/min/mL) and relative ^{99m}Tc-tetrofosmin uptake in normal and metabolism-perfusion mismatch (MMPM) regions. ^{99m}Tc-tetrofosmin uptake values are normalized to respective patient's maximum uptake region, set as 100%. Significantly reduced uptake of ^{99m}Tc-tetrofosmin in the MPMM region was shown to maintain absolute MBF as assessed with ^{15}O-water PET. Figure is from the reference (35) with modification.

tetrofosmin is utilized as a flow tracer. As long as the trapping mechanism is related to the membrane potential and mitochondrial integrity, alteration in energy-related processes can contribute to the reduction of the equilibrium concentration of ^{99m}Tc-tetrofosmin in tissue.

In the work by Schaefer et al. (35), SPECT images were acquired at approximately 1 hour after the ^{99m}Tc-tetrofosmin administration. This timing was empirically determined to provide improved contrast in the myocardium relative to liver rather than to maintain the linearity between the tracer concentration and the true flow (32). Earlier SPECT scans, when clearance of ^{99m}Tc-tetrofosmin is less significant, would have been more suited for providing images proportional to the perfusion like in the protocol employed for ^{201}Tl. While the assumption of microsphere-like behavior may be reasonable for early imaging times in normal myocardium, delayed imaging, particularly in the MPMM regions, no longer only reflects regional perfusion. The findings should be taken as an opportunity to elucidate additional information about the underlying processes. Vanoverschelde et al. (36) demonstrated that the resting blood flow could be normal in hibernating myocardium of patients with old myocardial infarction, in which coronary flow reserve was reduced. Preserved resting flow in the MPMM regions reported in the work of Schaefer et al may therefore not be surprising. Similar methodology employed for $H_2{}^{15}O$ PET could be applied to ^{99m}Tc-tetrofosmin SPECT for better understanding of pathophysiology in such regions. A mathematical-model based kinetic analysis could be useful for simultaneously estimating both flow and the effects of membrane potential and mitochondrial integrity.

Technical factors

There have been several concerns related to technical limitations of SPECT quantification. One essential factor was the mismatch between the X-ray CT-derived attenuation maps and the emission data. Respiration-induced movement is obvious, and the CT acquisition does not necessarily provide an appropriate attenuation map in PET/CT (37) or in SPECT/CT (38, 39). Efforts have been made to minimize errors attributed to the mis-registration between the emission and CT (40), by visualizing and controlling the breathing depth of the subject, which allows determination of the exact breath-hold phase for each subject. However this technique is dependent on patient cooperation and is difficult to apply in practice. More recently, techniques have been proposed to non-linearly register an attenuation map obtained from cine-CT to respiratory gated PET or SPECT data (41). Despite the availability of techniques that reduce x-ray exposure in the CT acquisition. There remain concerns in the use of cine-CT. It should also be noted that adequacy of such techniques need to be validated for a large clinical population. Similarly, natural motion of the patient can cause errors, unless a sophisticated fixation system is adopted, though this is more difficult than in brain PET and SPECT examinations. The partial volume effects which are caused by poorer spatial resolution relative to thickness of the walls, and also by the contractile motion are essential source of errors, which need further sophisticated methodologies. The automatic registration of attenuation map and emission data via algorithms that incorporate joint registration and reconstruction has recently been demonstrated for PET/CT (42). Although this approach has not yet been demonstrated for SPECT/CT the approach would be attractive for future clinical application.

Impact of high-sensitivity, fast-dynamic SPECT

Recently, high-sensitivity solid state SPECT systems have become clinically available. GE Healthcare use a stationary set of 19 Cadmium Zinc Telluride (CZT) detectors, each with pinhole collimators that is focused on a fixed region where the patient's heart must be manually located, improving the sensitivity to cardiac counts (effectively sensitivity is improved by a factor of 3). CZT detectors have excellent energy resolution and high counting rate performance. Coupled with the stationary geometry the system is ideal for dynamic acquisition. A further CZT system was introduced by Spectrum Dynamics (D-SPECT) in which 9 detectors rotate on their own axes covering the whole field-of-view. The system is designed to preferentially acquire counts from the myocardial area using an interactive user-selected region, resulting in a high sensitivity for myocardial counts, similar to that achieved on the GE camera (43). For fast dynamic studies, images are reconstructed from list mode data acquired for

limited projection angles that correspond to the cardiac region only, resulting in truncation of the field-of-view. A careful analysis (44) demonstrated that the reconstructed images were essentially consistent with those obtained from a conventional SPECT system acquired with 180° views, but with better image quality (superior noise properties). It was claimed that, by taking the left-ventricular radioactivity curve as an input function, coronary flow reserve (CFR) can be estimated from adenosine stress-to-rest ratio of influx rate constants (K_1) for ^{99m}Tc-sestamibi, which resulted in CFR values ranging from 1 to 2 fold in a heterogeneous patient population of cardiovascular diseases (45). The Possibility of quantitative measurement of MBF was also mentioned in a recent article of Miyagawa (46) using semiconductor SPECT systems. Image quality was in fact shown to be superior to that of conventional SPECT systems, even under the presence of the truncation in the acquired data. Note however that corrections were not performed for attenuation or scatter. The results of this study reported that the coronary flow reserve was lower in patients with perfusion defects and in regions supplied by stenotic coronary arteries. Regional flow values cannot be estimated due to the lack of absolute quantification, however, CFR values were obtained, assuming that both rest and stress measurements have similar proportionality to absolute flow. Estimated CFR clearly has several potential sources of error, especially the lack of attenuation and scatter correction, but also there is concern regarding the accuracy of the interior reconstruction, attributed to greater amount of attenuation and lack of a projection coverage (47). Several researchers have studied reconstruction for an interior region and demonstrated feasibility for X-ray CT [e. g. (47)]. However little is understood in the case of SPECT, especially when attenuation correction is omitted. Further investigation is clearly required.

Conclusions

The power of radiotracer imaging techniques, such as PET and SPECT, lies in their ability to trace physiological processes and biochemical pathways. Use of dynamic tracer information is well established in PET for quantifying particular physiological and biochemical processes of interest. The limited sensitivity and resolution of SPECT and the traditional lack of quantitative studies with SPECT due to attenuation and scatter correction limitations have popularized SPECT tracers with relatively slow kinetics, where qualitative images of perfusion could be obtained by static SPECT imaging. Furthermore, imaging and processing protocols have frequently been tailored to improve the perceived quality of the images, such as delaying acquisition to allow clearance of tracer from adjacent liver. However, tracer uptake at a given time point is rarely only governed by a single process such as flow, but by a number of mechanisms including blood flow, transport mechanisms across capillaries and cell membranes and binding and retention in the cells. With the exception of early and delayed redistribution imaging of ^{201}Tl, little advantage has been taken of the potential additional information obtainable from following the time course of tracer in the tissue. Quantitative reconstruction should be able to overcome these problems, but with expense of prolonged scan time. The recently introduced high-sensitive SPECT systems contribute to reduce the acquisition period or to reduce radiation exposure for static imaging. These systems are attractive for dynamic studies as they can acquire fast frame-rates with higher counting rates than conventional SPECT systems. However there is definite need for inclusion of methods for attenuation and scatter correction on these systems and validation of quantitative performance. Development of novel ligands ideal for quantitative assessment for myocardial blood flow would then be needed.

Acknowledgments

This article publication was supported by a Grant from Strategic Basic Research Programs, Agency for Medical Research and Development (AMED), Japan, a Grant for Translational Research from the Ministry of Health, Labour and Welfare (MHLW), Japan, and Japan Cardiovascular Research Foundation. BFH is supported by the UK National Institute of Health Research University College London Hospitals Biomedical Research Centre.

Sources of funding

None

Conflicts of interest

HI receives research grant from Nihon Medi-Physics. Other coauthors nothing to declare.

Reprint requests and correspondence:
Hidehiro Iida, PhD, DSc
Department of Investigative Radiology, National Cerebral & Cardiovascular Research Center - Research Institute, 5-7-1 Fujishiro-dai, Suita City, Osaka, Japan 565-8565
E-mail: iida@ri.ncvc.go.jp

References

1. Rosenthal MS, Cullom J, Hawkins W, et al. Quantitative SPECT imaging: a review and recommendations by the Focus Committee of the Society of Nuclear Medicine Computer and Instrumentation Council. J Nucl Med 1995; 36: 1489-513.
2. Iida H, Eberl S. Quantitative assessment of regional myocardial blood flow with thallium-201 and SPECT. J Nucl Cardiol 1998; 5: 313-31.
3. Iida H, Nakagawara J, Hayashida K, et al. Multicenter

evaluation of a standardized protocol for rest and acetazolamide cerebral blood flow assessment using a quantitative SPECT reconstruction program and split-dose ^{123}I-iodoamphetamine. J Nucl Med 2010; 51: 1624-31.
4. Yoneda H, Shirao S, Koizumi H, et al. Reproducibility of cerebral blood flow assessment using a quantitative SPECT reconstruction program and split-dose ^{123}I-iodoamphetamine in institutions with different gamma-cameras and collimators. J Cereb Blood Flow Metab 2012; 32: 1757-64.
5. Tossici-Bolt L, Hoffmann SM, Kemp PM, et al. Quantification of [^{123}I] FP-CIT SPECT brain images: an accurate technique for measurement of the specific binding ratio. Eur J Nucl Med Mol Imaging 2006; 33: 1491-9.
6. Varrone A, Dickson JC, Tossici-Bolt L, et al. European multicentre database of healthy controls for [^{123}I] FP-CIT SPECT (ENC-DAT): age-related effects, gender differences and evaluation of different methods of analysis. Eur J Nucl Med Mol Imaging 2013; 40: 213-27.
7. Buchert R, Kluge A, Tossici-Bolt L, et al. Reduction in camera-specific variability in [^{123}I] FP-CIT SPECT outcome measures by image reconstruction optimized for multisite settings: impact on age-dependence of the specific binding ratio in the ENC-DAT database of healthy controls. Eur J Nucl Med Mol Imaging 2016; 43: 1323-36.
8. Onishi Y, Yonekura Y, Nishizawa S, et al. Noninvasive quantification of iodine-123-iomazenil SPECT. J Nucl Med 1996; 37: 374-8.
9. Iida H, Eberl S, Kim KM, et al. Absolute quantitation of myocardial blood flow with ^{201}Tl and dynamic SPECT in canine: optimisation and validation of kinetic modelling. Eur J Nucl Med Mol Imaging 2008; 35: 896-905.
10. Narita Y, Iida H. Scatter correction in myocardial thallium SPECT: needs for optimization of energy window settings in the energy window-based scatter correction techniques. Kaku Igaku 1999; 36: 83-90.
11. Di Bella EV, Ross SG, Kadrmas DJ, et al. Compartmental modeling of technetium-99m-labeled teboroxime with dynamic single-photon emission computed tomography: comparison with static thallium-201 in a canine model. Invest Radiol 2001; 36: 178-85.
12. Smith AM, Gullberg GT, Christian PE, et al. Kinetic modeling of teboroxime using dynamic SPECT imaging of a canine model. J Nucl Med 1994; 35: 484-95.
13. Smith AM, Gullberg GT, Christian PE. Experimental verification of technetium 99m-labeled teboroxime kinetic parameters in the myocardium with dynamic single-photon emission computed tomography: reproducibility, correlation to flow, and susceptibility to extravascular contamination. J Nucl Cardiol 1996; 3: 130-42.
14. Lau CH, Eberl S, Feng D, et al. Optimized acquisition time and image sampling for dynamic SPECT of Tl-201. IEEE Trans Med Imaging 1998; 17: 334-43.
15. de Silva R, Yamamoto Y, Rhodes CG, et al. Preoperative prediction of the outcome of coronary revascularization using positron emission tomography. Circulation 1992; 86: 1738-42.
16. Iida H, Kanno I, Takahashi A, et al. Measurement of absolute myocardial blood flow with $H_2{}^{15}O$ and dynamic positron-emission tomography. Strategy for quantification in relation to the partial-volume effect. Circulation 1988; 78: 104-15.
17. Iida H, Rhodes CG, de Silva R, et al. Myocardial tissue fraction-correction for partial volume effects and measure of tissue viability. J Nucl Med 1991; 32: 2169-75.
18. Yamamoto Y, de Silva R, Rhodes CG, et al. A new strategy for the assessment of viable myocardium and regional myocardial blood flow using ^{15}O-water and dynamic positron emission tomography. Circulation 1992; 86: 167-78.
19. Iida H, Itoh H, Nakazawa M, et al. Quantitative mapping of regional cerebral blood flow using iodine-123-IMP and SPECT. J Nucl Med 1994; 35: 2019-30.
20. Iida H, Itoh H, Bloomfield PM, et al. A method to quantitate cerebral blood flow using a rotating gamma camera and iodine-123 iodoamphetamine with one blood sampling. Eur J Nucl Med 1994; 21: 1072-84.
21. Iida H, Akutsu T, Endo K, et al. A multicenter validation of regional cerebral blood flow quantitation using [^{123}I]iodoamphetamine and single photon emission computed tomography. J Cereb Blood Flow Metab 1996; 16: 781-93.
22. Kim K, Watabe H, Hayashi T, et al. Quantitative Mapping of Basal and Vasareactive Cerebral Blood Flow using Split-Dose ^{123}I-Idoamphetamine and Single Photon Emission Computed Tomography. Neuroimage 2006; in press.
23. Koshino K, Fukushima K, Fukumoto M, et al. Quantification of myocardial blood flow using ^{201}Tl SPECT and population-based input function. Ann Nucl Med 2014; 28: 917-25.
24. Maruno H. [Adquacy evaluation of quantitative reconstruction and compartment-model based MBF assessment]. Final Report of Grant for Translational Research from the Ministry of Health, Labor and Welfare (MHLW), Japan H19-Trans-G001 2009. p.194-6.
25. Iida H, Nakagawara J, Hatazawa J, et al. Estimation of the arterial blood radioactivity concentration using the whole body-to-arterial blood partition coefficients and the cross-calibration factor in ^{123}I-iodoamphetamine SPECT-towards a noninvasive clinical protocol with the QSPECT-DTARG method. Kaku Igaku 2012; 49: 49-58.
26. Sugihara H, Yonekura Y, Kataoka K, et al. Estimation of coronary flow reserve with the use of dynamic planar and SPECT images of Tc-99m tetrofosmin. J Nucl Cardiol 2001; 8: 575-9.
27. Arbab AS, Koizumi K, Toyama K, et al. Ion transport systems in the uptake of ^{99}Tc^{m}-tetrofosmin, ^{99}Tc^{m}-MIBI and ^{201}Tl in a tumour cell line. Nucl Med Commun 1997; 18: 235-40.
28. Arbab AS, Koizumi K, Toyama K, et al. Technetium-99m-tetrofosmin, technetium-99m-MIBI and thallium-201 uptake in rat myocardial cells. J Nucl Med 1998; 39: 266-71.
29. Younes A, Songadele JA, Maublant J, et al. Mechanism of uptake of technetium-tetrofosmin. II: Uptake into isolated adult rat heart mitochondria. J Nucl Cardiol 1995; 2: 327-33.
30. Spadafora M, Cuocolo A, Golia R, et al. Effect of trimetazidine on ^{99}Tc^{m}-tetrofosmin uptake in patients with coronary artery disease. Nucl Med Commun 2000; 21: 49-54.
31. Higley B, Smith FW, Smith T, et al. Technetium-99m-1,2-bis [bis(2-ethoxyethyl) phosphino] ethane: human biodistribution, dosimetry and safety of a new myocardial perfusion imaging agent. J Nucl Med 1993; 34: 30-8.
32. Jain D, Wackers FJ, Mattera J, et al. Biokinetics of technetium-99m-tetrofosmin: myocardial perfusion imaging

agent: implications for a one-day imaging protocol. J Nucl Med 1993; 34: 1254-9.
33. Takeishi Y, Takahashi N, Fujiwara S, et al. Myocardial tomography with technetium-99m-tetrofosmin during intravenous infusion of adenosine triphosphate. J Nucl Med 1998; 39: 582-6.
34. Tanaka R, Nakamura T. Time course evaluation of myocardial perfusion after reperfusion therapy by ^{99m}Tc-tetrofosmin SPECT in patients with acute myocardial infarction. J Nucl Med 2001; 42: 1351-8.
35. Schaefer WM, Nowak B, Kaiser HJ, et al. Comparison of microsphere-equivalent blood flow (^{15}O-water PET) and relative perfusion (^{99m}Tc-tetrofosmin SPECT) in myocardium showing metabolism-perfusion mismatch. J Nucl Med 2003; 44: 33-9.
36. Vanoverschelde JL, Wijns W, Depre C, et al. Mechanisms of chronic regional postischemic dysfunction in humans. New insights from the study of noninfarcted collateral-dependent myocardium. Circulation 1993; 87: 1513-23.
37. Gould KL, Pan T, Loghin C, et al. Reducing radiation dose in rest-stress cardiac PET/CT by single poststress cine CT for attenuation correction: quantitative validation. J Nucl Med 2008; 49: 738-45.
38. Goetze S, Brown TL, Lavely WC, et al. Attenuation correction in myocardial perfusion SPECT/CT: effects of misregistration and value of reregistration. J Nucl Med 2007; 48: 1090-5.
39. Goetze S, Wahl RL. Prevalence of misregistration between SPECT and CT for attenuation-corrected myocardial perfusion SPECT. J Nucl Cardiol 2007; 14: 200-6.
40. Koshino K, Fukushima K, Fukumoto M, et al. Breath-hold CT attenuation correction for quantitative cardiac SPECT. EJNMMI Res 2012; 2: 33.
41. McQuaid SJ, Lambrou T, Hutton BF. A novel method for incorporating respiratory-matched attenuation correction in the motion correction of cardiac PET-CT studies. Phys Med Biol 2011; 56: 2903-15.
42. Bousse A, Pedemonte S, Thomas BA, et al. Markov random field and Gaussian mixture for segmented MRI-based partial volume correction in PET. Phys Med Biol 2012; 57: 6681-705.
43. Erlandsson K, Kacperski K, van Gramberg D, et al. Performance evaluation of D-SPECT: a novel SPECT system for nuclear cardiology. Phys Med Biol 2009; 54: 2635-49.
44. Sharir T, Ben-Haim S, Merzon K, et al. High-speed myocardial perfusion imaging initial clinical comparison with conventional dual detector anger camera imaging. JACC Cardiovasc Imaging 2008; 1: 156-63.
45. Ben-Haim S, Murthy VL, Breault C, et al. Quantification of myocardial perfusion reserve using dynamic SPECT imaging in humans: a feasibility study. J Nucl Med 2013; 54: 873-9.
46. Miyagawa M, Nishiyama Y, Tashiro R, et al. Novel cardiac SPECT technology with semiconductor detectors: emerging trends and future perspective. Ann Nucl Cardiol 2015; 1(1): 18-26.
47. Defrise M, Noo F, Clackdoyle R, et al. Truncated Hilbert transform and image reconstruction from limited tomographic data. Inverse Problems 2006; 22: 1037-53.
48. Knuuti J, Kajander S, Maki M, et al. Quantification of myocardial blood flow will reform the detection of CAD. J Nucl Cardiol 2009; 16: 497-506.
49. Weich HF, Strauss HW, Pitt B. The extraction of thallium-201 by the myocardium. Circulation 1977; 56: 188-91.